Evidence of Innovation

Steven E. Seltzer, MD, *Editor*

Molecular Basis of Magnetic Relaxation of Water Protons of Tissue

Seymour H. Koenig, PhD

The uncontested utility of magnetic resonance (MR) imaging in diagnostic medicine—its noninvasive character, its three-dimensional (3D) capability, its geometric versatility, the high contrast and resolution available in soft-tissue images, and its potential for imaging physiologic functions—are matters of serendipity. As is now generally known, MR images are generated by nuclear magnetism: the precessing magnetic moments of the protons of mobile water molecules of tissue [1–3]. Because the density of these protons varies little among different tissues, spatial variations of image intensity—at least to a first appoximation—are dominated by tissue-dependent values of 1/T1 and 1/T2 of tissue water protons. These are the parameters that characterize the rate at which the orientational distribution of the proton moments, once perturbed, returns to thermal equilibrium. Approximate values of 1/T1 and 1/T2 for a variety of tissues are known from early in vitro measurements [4], so that reasonable estimates for the contrast to be anticipated in MR imaging could be made in the early stages of its development. However, there is no way in which useful estimates of relaxation rates could have been deduced a priori from applying theory to those water–macromolecular interactions in tissue now known to induce proton relaxation.

It has been only in the past few years that the nature of these intermolecular interactions has been clarified and a quantitative understanding of relaxation achieved [5]. Briefly, relaxation depends on three realities: (1) Tissue water protons are relaxed predominantly during the time that water molecules are bound at the protein–water interfaces of cytoplasmic protein; (2) this binding is so heterogeneous that particular sites, covering less than 1% of the interfacial area, contribute almost all the observed relaxation; and (3) cytoplasmic protein of tissue is highly organized spatially, ostensibly in well-defined 3D groupings, such that the thermal (Brownian) rotational motion of individual protein molecules is highly restricted. This last point enhances the first point dramatically. The serendipity that makes MR imaging feasible is the unexpected existence of a minority of water-binding sites with highly favorable relaxation-inducing properties, which in turn relate to the organization and immobility of the majority of cytoplasmic protein. When inserted into 50-year-old theory of relaxation of one proton by another [6], these realities—together with the well-founded assumption that water molecules are free to diffuse throughout tissue essentially unimpeded until they physically collide with cytoplasmic protein [2])—lead to a molecular-level, quantitative description of proton relaxation in tissue. However, the fundamental empirical finding—the dominant role of transfer of magnetic energy between the protons of water and the protons of tissue protein—has been used empirically, and to advantage, to clarify relaxation in protein solutions [7] and to account for magnetization transfer in MR imaging [8, 9]. It is the mechanistic description at the molecular level that is new.

The evolution of the understanding of the origin of contrast in MR imaging is akin to that of genetics in the 1960s. It is fair to say that before the insights of Watson and Crick regarding base pairing in DNA, the molecular

From Relaxometry, Inc., Mahopac, NY, and the Department of Radiology, Dartmouth–Hitchcock Medical Center, Hanover, NH.

Address reprint requests to S. H. Koenig, PhD, Relaxometry, Inc., P.O. Box 760, Mahopac, NY 10541.

Received November 17, 1995, and accepted for publication after revision March 11, 1996.

Acad Radiol 1996;3:597–606

basis of genetics was unknown, whereas immediately after genetics was essentially understood. It was the end of a mystery but the beginning of the new era of molecular genetics. Similarly, before 1993, the molecular basis of water proton relaxation in tissue was unknown, whereas now it is understood in quantitative detail [5]. By analogy, this new understanding, too, can be the start of an era in which 1/T1 and 1/T2 of both normal and diseased tissue can be related, quantitatively, to events in tissue at the molecular level [10–12] to further the diagnostic (and potential prognostic) capabilities of MR imaging as it is currently used and to provide insights into functional imaging. In this article, the fourth of related articles [1–3], I put current understanding into historical perspective.

I emphasize the basic mechanisms that contribute to water proton relaxation in all types of tissue but that are applicable directly to relatively homogeneous tissue with minimal lipid content (e.g., liver, spleen, gray matter). For white matter, a more heterogeneous tissue, the lipid protons of myelin provide an additional relaxation contribution for the MR imaging–visible water protons. The responsible mechanism [13, 14] was identified before the more universal mechanisms were understood [5]. By contrast, the lipids of adipose tissue contribute an additive signal in MR imaging [1], ostensibly with little interference with the water proton signal or its relaxation. Calcifications also add another mechanism to tissue water proton relaxation, which was recognized only recently [11, 12], and iron from hemorrhage [10, 11] may as well. In particular, "old iron" in the brain, when sequestered in ferritin or hemosiderin, dominates 1/T2 of the brain in some instances [15], but it may not contribute significantly to 1/T1. These "add-ons," however, are not my immediate concern.

HISTORICAL DEVELOPMENT

Phenomenology of Relaxation in Protein Solutions and Tissue

Figure 1 shows the current phenomenology of relaxation of tissue water protons. The solid symbols in Figure 1A [16] show the magnetic field dependence (the nuclear magnetic relaxation dispersion [NMRD] profile) of 1/T1 of four samples of human tissue: three normal (muscle, spleen, and lung) and one abnormal (astrocytoma). The solid curve through the data for muscle is an empirical fit [2]; the three dashed curves are scaled from the solid curve by a constant (with a small correction for water background). Certainly, to first order,

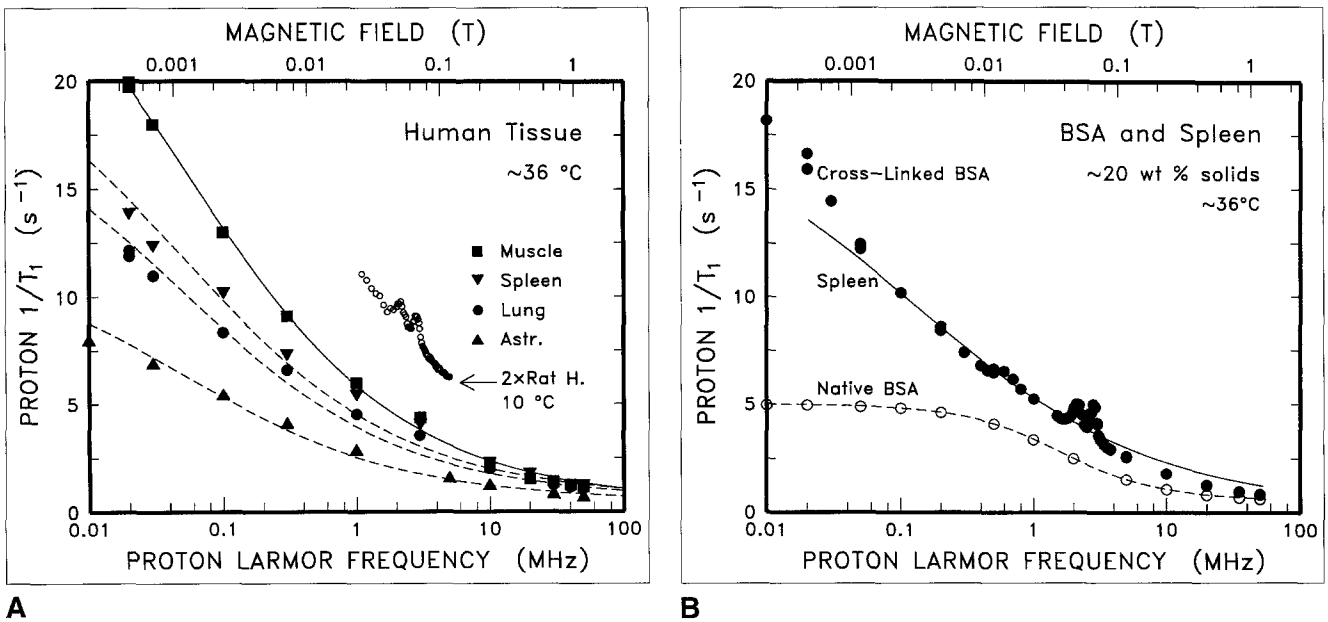

FIGURE 1. ***A***, 1/T1 of water protons for four samples of human tissue: three normal (muscle, spleen, and lung) and one abnormal (astrocytoma [Astr.]) [16]. The solid curve through the data for muscle is an empirical fit to the data [2]; the three dashed curves are scaled from the solid-line curve by a constant (with a small correction for water background). The open symbols, an enlarged detail of a part of the profile of the rat heart (H) at 10°C [17], are included to show peaks in 1/T1 that are universally present in tissue. ***B***, 1/T1 nuclear magnetic relaxation dispersion profiles of water protons of three samples with the same protein content (20 wt%), near physiologic temperature: the human spleen data in ***A*** (*solid curve*), native bovine serum albumin (BSA; *open circles*), and the same sample with the protein immobilized by cross-linking with glutaraldehyde (*solid symbols*) [5, 16].

these four profiles have the same functional dependence on magnetic field (B_0) differing only by a tissue-dependent (but, unfortunately, not tissue-specific), multiplicative constant. The open symbols, depicting an enlarged area of the profile of rat heart at 10°C [17], are included to show peaks in 1/T1 that are universally present in tissue [10–12] but time-consuming to measure [17].

Figure 1B shows NMRD profiles of three samples that all contain ~20 wt% protein: the human spleen data from Figure 1A (solid curve), a water solution of native bovine serum albumin (BSA; open circles and dashed curve), and the native sample with its protein chemically cross-linked (filled circles). It is now known that a sample of immobilized protein in water is such a good phantom for homogeneous tissue (i.e., excluding white matter and adipose tissue) that one cannot be distinguished from the other from measurements of relaxation rates. This is true whether one measures 1/T1, 1/T2, 1/T1ρ, or magnetization transfer, at any value of static or radiofrequency magnetic field, and at any temperature, and whether these measurements are made with an imager or a relaxometer. Moreover, the 1/T1 NMRD profiles of protein are the same regardless of whether the latter is immobilized by chemical cross-linking (as in Fig. 1B), thermal denaturation (cooked egg whites [3]), physical crowding at high concentrations (the low-density, eye-lens protein α-crystallin [18]), polymerization (deoxysickle hemoglobin [19]), or drying to a hydrated powder [5].

Much of what is now known about the profiles of solutions of native, rotationally mobile protein (Fig. 1B) has been known for some time [16]: In what is thought to be the first reported 1/T1 NMRD profile of a native protein (demetalated transferrin, in 1969 [20]), a comparison of the data with the basic concepts of relaxation theory showed that the profiles could be explained only if "a small fraction of the number [of water molecules] usually considered to be in the first hydration shell . . . with lifetimes . . . in the range 0.1 to 10 μs" were bound in such a way as to sense the Brownian rotation of the solute protein molecules. Subsequent exchange conveys this information to all solvent protons. In particular, the inflection of the profile for native BSA near 3 MHz (Fig. 1B) reflects the rate of Brownian reorientation of the solute molecules; it moves to lower fields for larger proteins, in inverse proportion to protein molecular weight (Fig. 4 in Koenig and Brown [16]). Also, the view, then and now, is that the dominant effect of the binding of water to protein relates to the temporary slowing of the motion of water molecules; the interaction of the protons of bound water with protein protons (magnetization transfer), although known to contribute somewhat to the native profiles [16], was not of fundamental importance. What was and is significant is that the functional form of the 1/T1 profiles for solutions of native protein, their dependence on molecular weight and temperature, and the anticipated 1/T2 profiles (which are much more difficult to measure) all were consistent with the basic formal aspects of the theory of relaxation in liquid solutions. However, the special nature of the "small fraction" of the hydration shell remained unknown for more than 20 years, until 1993 [5].

The major empirical distinctions in functional form between the profiles of native and immobile protein was first considered in a discussion of concepts current in 1988 [3]. In addition to the obvious difference in dependence on B_0 (Fig. 1B), peaks appear in the profile for immobile protein (as for the rat heart; Fig. 1A), two larger ones near 2.2 and 2.8 MHz and a smaller one at the difference frequency of 0.6 MHz [17]. (These peaks were not considered earlier [3].) In addition, the temperature sensitivity of the profiles was known to be significantly reduced by immobilization, and the high-field value of 1/T2 becomes similar to the low-field value of 1/T1 rather than to 0.3 of the low-field 1/T1. These aspects of the NMRD profiles, as well as the relaxation rate peaks, also are characteristic of tissue [5, 10–12]. Indeed, at the time of that discussion [3], the phenomenologic resemblance between the NMRD profiles of tissue and immobile protein was well established. What was not understood then were (1) the source of the heterogeneity of water binding at a typical protein–water interface, which involves multiple hydrogen-bond formation; (2) that the mobile–immobile protein NMRD transition relates to a switch from liquidlike to solid state–like behavior of the relaxation of protein protons; and (3) that immobilization enhances the transfer of magnetic energy between solute and solvent protons. Indeed, the current understanding came about during the period that magnetization transfer contrast imaging was first proposed [21].

Today, there is a a quantitative theoretical understanding of all aspects of the NMRD profile of cross-linked BSA [1] (Fig. 1B) and, by extension, of the origin of contrast in MR imaging. Before expanding on this, it is necessary to recount the major concepts underlying the relaxation of protons in liquids and solids.

Theory of Relaxation in Protein Solutions and Tissue

Longitudinal relaxation of two interacting ensembles of protons. Assume that δW is the (time-dependent) fractional deviation of the magnetization of tissue water protons from their thermal equilibrium value and that δP is that of the protons of tissue macromolecules (assumed to be mostly protein). Further assume that each of these ensembles has its own intrinsic relaxation rates, R_W and R_P, in the absence of transfer of magnetization between the two ensembles. (Here R_W includes all influences of the protein on the relaxation rate of water other than magnetization transfer, such as from paramagnetic ions or alteration of solvent hydrodynamics, as well as contributions from solute contrast agents.) If these assumptions are true, then the most general formulation of their joint relaxation (assuming linear behavior)—the pair of phenomenologic differential equations that describes their coupled evolution in time for all experimental conditions—is as follows [5, 7–9]:

$$d(\delta W)/dt = -R_W(\delta W) - \sigma[(\delta P) - (\delta W)]$$
$$d(\delta P)/dt = -m\sigma[(\delta W) - (\delta P)] - R_P(\delta P)\ . \quad (1)$$

Here, σ characterizes the rate of transfer of magnetization from protein to water when the protein and water ensembles deviate from equilibrium by different fractional amounts, and m is the ratio of the number of water to protein protons (i.e., the relative magnetic energy in the two ensembles at equilibrium). (σ is identical to $-K$ as measured in magnetization transfer contrast [21].) It is often useful to rewrite these equations in terms of the deviations of each ensemble from its own equilibrium:

$$d(\delta W)/dt = -\lambda_W(\delta W) - \sigma(\delta P)$$
$$d(\delta P)/dt = -m\sigma(\delta W) - \lambda_P(\delta P)\ , \quad (2)$$

where $\lambda_W = R_W - \sigma$ and $\lambda_P = R_P - m\sigma$.

The general solution of this pair of linear differential equations is a biexponential decay for both δW and δP, with the same two characteristic "eigenrates" for each but with different relative magnitudes of the two components [5]. At typical MR imaging fields, the faster rate characterizes the magnetization transfer between water and protein; the slower one characterizes the relaxation of the combined magnetizations of the two ensembles. Under typical experimental conditions, for both MR imaging and NMRD, the slower decay rate is the one that is measured and identified with 1/T1. In magnetization transfer contrast experiments, the magnetization of the protein spins is saturated by off-resonance irradiation (bringing them to an "infinite spin temperature"), so that the time dependence of δP in equations 1 and 2 is eliminated. The result is that δW varies as a single exponential with decay rate λ_W.

These equations can be invoked at two levels: the macroscopic level, where the three unknown rates R_W, R_p, and σ are fit to defining experiments so that their values then can be used to predict further results in altered circumstances, or the molecular level, where they can be related to molecular parameters if a mechanistic model is available. At the macroscopic level, these equations have been used in some detail in studies of magnetization transfer contrast [8, 9]. At the molecular level, from NMRD studies the same equations have been used to determine the density and characteristics of the water-binding sites at the protein–water interface in tissue [5].

Thermal rotational motion of water molecules and relaxation in liquids. A few years after the discovery of nuclear MR in solids and liquids in 1945 [22, 23], the theoretical concepts of proton relaxation in liquids were clarified [6]: In liquid water, protons are relaxed by other protons, mostly through intramolecular interactions between the magnetic dipoles of the two protons of a single water molecule. This interaction is large and causes a precession of one proton in the field of the other at a rate 10^5 radians sec^{-1} (corresponding to a period of ~10 μsec). It also is a function of the spatial orientation of the water molecule. The thermally induced Brownian rotation of a water molecule proceeds at a much greater rate: 2×10^{10} radians sec^{-1} at 25°C. This rapid modulation of the relaxation-inducing interaction tends to minimize its effect. The net result is a "motional narrowing" of the intramolecular interaction [1], which increases its characteristic interaction period, 10 μsec, by a factor of $2 \times 10^{10}/10^5$ to give a relaxation time of ~2 sec. The observed time at 25°C is 4 sec. The more formal aspects of relaxation theory are concerned with quantifying the concept of motional narrowing and deriving the dependence of relaxation rates on B_0 (i.e., showing how proton precession influences motional narrowing to generate 1/T1 and 1/T2 NMRD profiles).

Note that proton relaxation relates to the mechanisms by which protons sense the surrounding temperature, mechanisms by which, ultimately, the magnetic (Zeeman) energy of these protons achieves thermal equilibrium. These require randomness (i.e., thermally driven fluctuations)—no fluctuations means no relaxation. Finally, for liquids, 1/T1 and 1/T2 are closely related [6];

in fact, they are different components of intrinsically directionally dependent relaxation rates. At low values of B_0, in liquids, when all directions become equivalent, 1/T1 and 1/T2 become equal. At large values of B_0, 1/T1 approaches zero, whereas 1/T2 approaches 0.3 of the low-field value of 1/T1. The relevance to MR imaging is that the binding of water molecules at the interface of stationary protein can slow the rotational motion of water molecules 10^6-fold. Thus, if a typical water molecule is in contact with tissue protein for one part in 10^4 of the time (a reasonable estimate), its relaxation rate can be enhanced 100-fold.

Relaxation in solids. Solids are rigid, and Brownian rotation of individual molecules of the solid is minimal, as, for example, in ice. As a result, 1/T1 and 1/T2 become unrelated conceptually. The longitudinal (parallel to B_0) relaxation rate, 1/T1, is still a measure of the time it takes for the magnetic energy to attain thermal equilibrium. It can become exceedingly long—no (rotational) fluctuations and, as a result, no relaxation. The transverse relaxation rate, 1/T2, is now uncoupled from, and unrelated to, 1/T1. The interaction of a proton with its neighbor is no longer motionally narrowed, so that a given proton will reorient (i.e., "flip") in the field of its neighbor in ~10 μsec, which is the interaction period. This "uncertainty" time is now T2 and is observable as the line width of the nuclear MR signal from protein protons found in magnetization transfer imaging [21]. A proton will not flip back in any coherent way because of the complexity of the system (i.e., the multiplicity of interproton interactions present). As a result, its initial spin orientation, when different from its neighbors, will propagate throughout the solid, which is akin to molecular diffusion in a concentration gradient. This process is called "spin diffusion." The net effect is that magnetic energy diffuses rapidly (a few milliseconds to traverse an immobile protein molecule) without loss. To first order, relaxation of Zeeman energy will occur only at specialized sites that can provide locally fluctuating magnetic fields; these become the sinks and sources of magnetic energy and contribute to 1/T1.

There is no analogous long-range spin diffusion in liquids. Rather, each mutual spin flip can both transport spin and relax Zeeman energy (because of fluctuations), so that spin diffusion does not progress beyond a few intermolecular distances. (On the other hand, chemical diffusion in low-viscosity liquids will transport magnetic energy with a diffusion rate that is 10^6-fold greater than spin diffusion in solids.) Finally, for protein protons, the transition from motionally narrowed, liquid-state conditions to solid state relaxation—which sets in when the rate of Brownian reorientation of the protein is comparable to the precession of a protein proton in the fields of its neighbor—occurs at a protein molecular mass of approximately 50,000,000 Da, which is far greater than that of any native protein unless it is immobilized by its cytoplasmic environment.

Heterogeneity of Binding of Water to Proteins in Solution

The current view [5, 24] is that water molecules are held at protein–water interfaces by single and multiple hydrogen bonds. To first order, their binding energies are additive, so that each additional bond increases the dissociation lifetime of a bound water molecule by the same factor: ~50 at 25°C. Water molecules held by four bonds have a lifetime of 1 μsec, as deduced recently from a comparison of deuteron 1/T1 NMRD profiles of native and cross-linked BSA [5, 24]. As might be anticipated, the interfacial density of these sites is low because the stereochemical requirements are so restrictive. An example of this would be a water molecule with one proton bonded symmetrically to the two oxygen molecules of an interfacial carboxylate and the other bonded symmetrically to nitrogen molecules of two interfacial histidines, as identified by neutron diffraction measurements of myoglobin crystals [25].

Other configurations have been suggested [5]. These are the binding sites hinted at in the first reported NMRD profiles of protein solutions [20] (quoted earlier). For BSA, there are two per hydration layer of ~700 water molecules. Judging from the NMRD profiles of many proteins and tissues, this surface density ranges over a factor of 2, a fact that explains the twofold range of 1/T1 and 1/T2 of tissue (Fig. 1A). For immobile protein and tissue, the 1-μsec lifetime—a long time for the present purposes—modulates the intramolecular interaction of the proton of a bound water molecule and its interaction with protein protons.

Three-bond sites also have been identified, as have two- and single-bond sites. The associated densities, lifetimes, and "correlation" frequencies (near which they contribute to the dependence of the profiles on B_0) are listed in Table 1 [24]. In general, the density of the more populous sites does not increase as rapidly as the lifetime decreases, so that all the NMRD profiles of tissue are dominated by the 1-μsec sites.

CURRENT CONCEPTS

The Six Parameters of Theory

Figure 2 [5] shows the proton 1/T1 NMRD profiles of two samples of chemically cross-linked BSA that are identical in all respects, except that the solvent was 100% protonated in one case and 90% deuterated in the other. (The spectral peaks, shown in Fig. 1B, have been omitted for clarity.) If the only proton–proton interactions of importance in relaxation were the intramolecular interactions in water, the shapes of the two profiles would be identical and the amplitude of that of the deuterated sample would be 10% of the undeuterated one. That this is not the case establishes immediately that interactions that transfer magnetization between solute and solvent protons dominate relaxation. The two solid curves associated with the data are the result of recent theory [5] applied to solvent interactions at a heterogeneous protein–water interface. They arise from a straightforward extension of earlier work on relaxation in two-spin systems [6] to derive expressions for α and the protein contribution to R_W (equation 1). R_P was obtained by a thorough reanalysis of early data on relaxation of protons in solid amino acids and protein, including remnant internal mobility [5]. Six phenomenologic parameters are involved in generating the two curves: (1) the density and lifetime of the 1-μsec, four-hydrogen-bond interfacial water-binding sites; (2) the density and lifetime τ_M of the 20-nsec, three-hydrogen-bond sites; and (3) the values of σ for the two classes of bound waters relative to the intramolecular proton–proton interaction in water. (The actual values used are 2 and 16 water molecules per BSA molecule, with lifetimes τ_M of 1 μsec and 23 nsec and relative interactions of 1 and 4.) From these, values for σ and R_W were computed, equation 1 solved for the eigenrates, which were substituted back into the equations to predict the observed 1/T1 NMRD profiles. The process was iterated, ultimately yielding the curved lines shown in Figure 2. The fit shows that 60% of the magnetization transfer funneled through the 1-μsec sites and that 40% funneled through the 20-nsec sites [15].

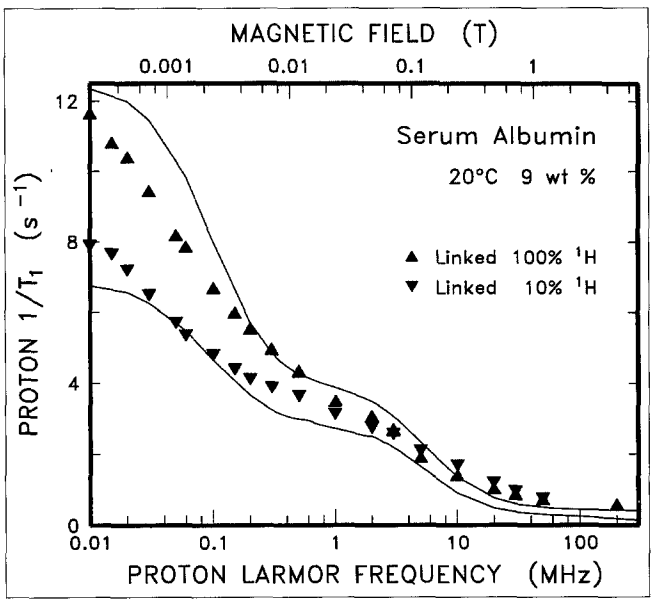

FIGURE 2. 1/T1 nuclear magnetic relaxation dispersion (NMRD) profiles of water protons of two samples of 9 wt% bovine serum albumin immobilized by cross-linking with glutaraldehyde at 20°C. The solvent water is undeuterated for the upper set of data points and 90% deuterated for the lower. The solid curves are derived from a six-parameter theory [5], of which four are known from deuteron NMRD profiles. The remaining two, the extent of magnetization transfer at the 1-μsec and 20-nsec sites, were adjusted to optimize the fit [5].

These six parameters also explain a great deal of the other data. First, if magnetization transfer is omitted (there is none between solvent deuterons and protein protons), and the magnitude of the deuteron magnetic moment is substituted for that of the proton, the theory predicts the observed deuteron 1/T1 profile of cross-linked BSA within experimental error [5]. Second, for native mobile BSA, the rotational relaxation time, and not τ_M, is the correlation time to be used in the computations. This yields the deuteron 1/T1 profile of native BSA within experimental error [5]. Thus, four of the six parameters—when inserted into theory [5]—are adequate to explain deuteron relaxation in native and cross-linked BSA. Therefore, the curves shown in Figure 2 may be regarded as having been generated by only two unknown parameters, with the remaining four derived from deuteron data. It is already known [26] that a mechanism not yet mentioned here affects the data as B_0 is lowered below ~0.05 MHz: the solid state–broadened energy levels of the protein protons begin to overlap, the distinction between spin-up and spin-down is lost, and any magnetization that crosses the interface from the solvent side is "short-circuited." Relaxation in the protein is immediate (10 μsec), and the influence of solute on solvent is limited by the magnetization transfer rate. This was not considered in generating the curves in Figure 2; its inclusion would improve the low-field agreement of data and theory.

Given the foregoing, including the fact that 3% or less of the protein–water interface has been invoked, plus the idealization that there is no heterogeneity within a given class of site (Table 1), I submit that the theoretical curves in Figure 2 are a remarkable two-parameter

TABLE 1: Approximate Lifetime τ_M of a Water Molecule Bound at a Protein–Water Interfacial Site When Held by *n* Hydrogen Bonds

n	τ_M (sec)	$\nu_c \approx 1/11\,\tau_M$ (MHz)	B_0 (Tesla)
4	1×10^{-6}	0.1	0.0024
3	2×10^{-8}	5	0.12
2	4×10^{-10}	250	6
1	8×10^{-12}	12,500	300

For solutions of immobilized protein, every value of τ_M determines a value of ν_c [20], the correlation frequency of a distinct dispersive contribution to the 1/T1 NMRD profiles of solvent protons, with an inflection at B_0. NMRD = nuclear magnetic relaxation dispersion.

characterization (both magnetization transfer parameters) of the observed proton 1/T1 NMRD profiles. In turn, these profiles are indistinguishable in form from those of most tissues, normal and abnormal [1, 10–12]. This means that the difference in MR imaging contrast between any two relatively homogeneous tissues (e.g., liver and spleen) always can be characterized by two parameters: the tissue-dependent densities of the recently discovered 1-μsec and 20-nsec sites, which relate to the protein composition and physical state of each tissue. All other aspects of relaxation are invariant and are the same as those that explain relaxation in solutions of immobilized protein. I now summarize the global picture.

Universal 1-μsec and 20-nsec Sites

With regard to the data in Figure 2, first consider the 0.1- to 1.0-MHz decade. The water molecules that dominate relaxation are those bound at the τ_M = 1 μsec, four-hydrogen-bond sites. The dynamic act of binding and unbinding generates fluctuations in the intramolecular water proton–proton interaction in the microsecond rather that the 20-psec regime, contributing so much to relaxation that only two bound water molecules per BSA suffice to account for the majority of 1/T1 and make MR imaging possible. The τ_M = 20 nsec sites, however, cannot be ignored. As already noted, the relative contributions of these two types of sites to magnetization transfer in BSA (and to 1/T2 at imaging fields [5]) is 2:1. (A cursory application of the data in Table 1 may suggest that this ratio should be higher; however, 1/T1 at low fields, as measured, is actually the slower of a biexponential variation, which must be extracted diligently from theory using equation 1 [5].) Given this, the fact that the profiles shown in Figure 1A scale by a single parameter implies that this ratio does not vary significantly from one tissue to another. However, an earlier compilation of many more tissue profiles (see Fig. 14 in Koenig [16]) implies, retrospectively, a variability in this ratio that should not be ignored.

Because the protons of the bound water molecules are in magnetic contact with protein protons, essentially all proton relaxation, as well as all magnetization transfer, takes place at these sites: For water protons, chemical diffusion brings the magnetic energy there and for protein protons, spin diffusion does the same. The dependence of 1/T1 on B_0 in this decade of field is as expected and is actually centered near 0.1 MHz, where the precession frequency is comparable to the inverse of $11 \times \tau_M$ [16, 20]. Were it not for the 20-nsec sites, 1/T1 would be close to zero for B_0 above ~1 MHz. The range of 1–40 MHz, the MR imaging range, is dominated by these three-bond sites. The recent realization of their existence [5] has made it possible to explain the two-decade-old profiles of a relatively large protein (450 kDa hemocyanin [2]). This profile, with an inflection at lower fields, has a second (but not obvious) dispersion above 1 MHz (analogous to that shown in Fig. 2) that is attributable to the 20-nsec sites and has remained unexplained until recently.

^{14}NH Peaks

The three peaks in the cross-linked BSA profile in Figure 1B are now readily explained. It has been known for some time that they are associated with the NH moieties of the protein and that their magnitude suggests that water protons can interact with the majority of them [17]. This would be difficult if it were not for interfacial magnetization transfer and spin diffusion throughout immobilized protein. The ^{14}N nuclei of the NH groups have electric quadrupolar moments; suffice it to say for now that there are nuclear levels at 2.2 and 2.8 MHz above a ground state with short relaxation times. Moreover, these levels are relatively independent of B_0. When B_0 is such that the proton energy (precession frequency) matches an energy difference between any two ^{14}N levels (0.6, 2.2, and 2.8 MHz), 1/T1 of the NH protons becomes large. These, in turn, become highly efficient relaxation sinks for proton magnetization diffusing in their vicinity, which gets reflected, ultimately, in the proton 1/T1 profile of solvent protons.

Relevance to 1/T2 at MR Imaging Fields

Above 40 MHz, the contribution of the 1-μsec and 20-nsec sites to 1/T1 of tissue becomes small, comparable

to the background rate of pure water and the contributions of adventitious oxygen and paramagnetic metal ions. The little relaxation that remains at typical imaging fields is, ironically, from the single- and double-hydrogen-bonded sites, which cover 97% of the protein–water interface [5, 20]. As a consequence, unless there is a specific contribution to 1/T1 from other sources (e.g., as already noted for the myelin of white matter [13, 14]), contrast in MR imaging must take advantage of tissue-dependent values of 1/T2. Fortunately, even when the macromolecular content of tissue is solidlike, its water remains mobile [2]. Therefore, motional narrowing theory is the proper description of relaxation, and—as a consequence—1/T2 at imaging fields, 0.3 of 1/T2 in the low-field limit, must mimic 1/T1 at low fields. This validates the use of 1/T1 NMRD data (Figs. 1B and 2) as a means of understanding the basis of contrast in MR imaging until 1/T2 profiles can be measured with comparable speed and accuracy.

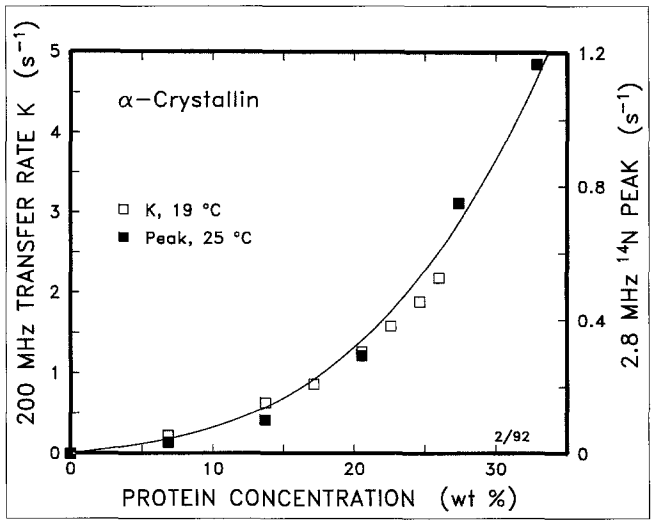

FIGURE 3. Variation with α-crystallin concentration of the magnetization transfer rate $K(= -\sigma$; equation 1) at 200 MHz (□) and the magnitude of the 2.8-MHz 1/T1 peak [17] (■), at 25°C. The relative vertical scales have been adjusted to emphasize the similar dependence of these two parameters. The smooth nonlinear curve associated with the data, which has only linear and cubic components, indicates a hydrodynamic interaction (crowding) between protein molecules.

A Remarkable Correlation

The foregoing, somewhat complex global view of proton relaxation in systems of rotationally restricted protein (including tissue) has made it possible to correlate two ostensibly unrelated sets of data measured for solutions of α-crystallin as a function of protein concentration [18]. Molecules of this highly soluble globular eye-lens protein are approximately 50% water, for reasons that enhance lens transparency, resulting in a molecular volume that is twice that expected from its molecular mass (800 kDa). As a result, protein–protein interactions at a given protein density are large, and the irreversible mobile–immobile transition of BSA (Fig. 1B) can be modeled reversibly using solutions of α-crystallin of varying concentrations [18]. In Figure 3, the dependence on protein concentration is plotted for two quantities, each of which—based on the view of proton relaxation in tissue—depend on magnetization transfer at the 1-μsec and 20-nsec sites. The nonlinearity of their dependence on protein concentration verifies that intermolecular interactions are significant at the concentrations shown; they slow solute rotation. One quantity is the height of the 2.8-MHz peak, which, provided that spin diffusion is adequate, will be proportional to the transfer rate at 2.8 MHz. The second is the rate of magnetization transfer measured using imaging techniques (at 200 MHz [18]), in which an off-resonance radio field is used to disequilibrate the spins of the protein protons. The resulting change in image intensity provides a measure of the rate of magnetization transfer, $K(= -\sigma)$, relative to the total 1/T1. Because B_0 is so high, the contribution of the long-lived sites is highly dispersed and, if additional mechanisms of magnetization transfer exist, then K at 200 MHz would not be expected to correlate with the height of the 2.8-MHz peak. This predicted correlation is shown in Figure 3; it is remarkably good and is not explicable outside of the global conception presented here.

CYTOPLASMIC ORDER AND CYTOPLASMIC CHAOS ORDER

Having argued, from the phenomenology of relaxation in tissue, that the majority of all cytoplasmic protein is immobilized [24], the next question is, Why, how, and to what extent? It is easy to say that it is obvious that cytoplasmic protein should be immobile: Cells have exoskeletons, which are extensive networks of membrane that can bind protein. However, the hemoglobin of red cells (which are really sacs of hemoglobin) is mobile despite the rigid macromolecular network that maintains the cells' shape, whereas the protein of hepatocytes (nucleated cells with complex functions) is not [2]. In addition, there is not enough lipid in most cells to fill the interstices between protein molecules if all cytoplasmic protein were assembled into a monolayer. Something more fundamental and

universal must be responsible, something that derives from an evolutionary need to optimize cell function. Previously, I [24] conjectured that the organization of protein in cells is an expression of a need for "cytoplasmic order," a 3D arrangement of cytoplasmic protein into functional groups, or clusters. Such groups (e.g., the proteins needed for electronic transport along a redox chain or those enabling the unfolding and threading of another protein through a mitochondrial membrane) could well be anchored to membranes or receptors at only a few points, with their rigid 3D organization maintained largely by specific protein–protein interactions. These would have evolved by the evolutionary fine-tuning of cellular, and tissue, function. As noted earlier, the clusters would have to be larger than 5×10^7 Da. I [24] also have argued that, for efficiency, these clusters should interfere minimally with each other because the cytoplasm is a crowded place. Thus, cytoplasmic protein of a normal cell, one that must perform a multiplicity of protein-mediated biochemical functions, must be highly organized and assembled into compact functional units, with each unit separated from the others for minimal mutual interference.

Chaos

If cytoplasmic order is fine-tuned for optimal functioning, what changes will occur in this order when cells become abnormal, in particular, neoplastic? In a recent study of 47 resected human astrocytomas [10], the most common malignant brain tumor in adults, a correlation was found between the amplitude of the NMRD profiles and the histologic grade of the tumor, a measure of aggressiveness. It is not straightforward to demonstrate this correlation because corrections must be made for variations in water content, and the unknown effects of hemorrhage and calcium deposits on 1/T1 [10–12] must be avoided. The results can be understood as a breakdown of cytoplasmic order, the onset of "cytoplasmic chaos." As cells become more transformed, different proteins will be expressed, the order needed for normal functioning will be compromised, and the factors that separate different clusters of protein will become ineffective. For fixed protein content, one expects more immobilization, greater relaxation rates, and more magnetization transfer. More data are needed to verify these conjectures. On the other hand, and consistent with the ideas of order and chaos, are the results for human meningiomas. These tumors, which are usually histologically benign, grow slowly. From the perspective of tissue water protons, they are physiologically similar to normal tissue and have little variability in their water contents and NMRD profiles [12].

THE FUTURE

In summary, the amplitudes of the proton 1/T1 NMRD profiles of tissue depend mainly on the amount of protein–water interfacial area in the cells, the densities of the three- and four-hydrogen-bond sites (the 20-nsec and 1-μsec sites), and the integrity of the spatial organization of cellular protein, something needed for normal cell function. This organization limits the rotational freedom of the protein, to which the amplitude of the profiles and the relative heights of the ^{14}NH peaks are highly sensitive. The information currently available is limited to fairly homogeneous tissue with relatively globular proteins. Little has been done with more complex tissues, such as cartilage, which is replete with fibrous collagen, and muscle; both cartilage and muscle have proteins with high surface-to-volume ratios. Will incipient loss of cartilage integrity (e.g., associated with arthritis), or the state of muscle in disease, show up in the more subtle details of its NMRD profiles? The compositions of many tissues are relatively constant over time, but many others are cyclic (e.g., hormone secretors). Will the secretory activity of such tissue, which involves time-dependent expression of different proteins, be reflected in their NMRD profiles? To go further, can the cycles of cell division in synchronized cell cultures be followed by NMRD methods? Finally, can compounds be found that compete with water for the 1-μsec sites? The average density of these sites in tissue is a few millimolar, which is comparable to the dosage used with paramagnetic contrast-altering agents. If so, there might be a class of diamagnetic agents yet to be discovered.

ACKNOWLEDGMENT

I thank Marga Spiller for a careful and constructive reading of the manuscript.

REFERENCES

1. Koenig SH, Brown RD III, Adams D, Emerson D, Harrison CG. Magnetic field dependence of 1/T1 of protons in tissue. *Invest Radiol* **1984**;19:76–81.
2. Koenig SH, Brown RD III. The importance of the motion of water for magnetic resonance imaging. *Invest Radiol* **1985**;20:297–305.
3. Koenig SH, Brown RD III. The raw and the cooked: or the importance of the motion of water for MRI, revisited. *Invest Radiol* **1988**;23:495–497.

4. Bottomly PA, Foster TH, Argersinger RE, Pfeifer, LM. A review of normal tissue hydrogen NMR relaxation times and relaxation mechanisms from 1-100 MHz: dependence on tissue type, NMR frequency, temperature, species, excision, and age. *Med Phys* **1984**;11:425–448.
5. Koenig SH, Brown RD III. A molecular theory of relaxation and magnetization transfer: Application to cross-linked BSA. A model for tissue. *Magn Reson Med* **1993**;30:685–695.
6. Solomon I. Relaxation processes in a system of two spins. *Phys Rev* **1955**;99:559–565.
7. Koenig SH, Bryant RG, Hallenga K, Jacob GS. Magnetic cross-relaxation among protons in protein solutions. *Biochemistry* **1978**;17:4348–4358.
8. Henkelman RM, Huang X, Xiang Q-S, Stanisz GJ, Swanson SD, Bronskill MJ. Quantitative interpretation of magnetization transfer. *Magn Reson Med* **1993**;29:759–766.
9. Morrison C, Henkelman RM. A model for magnetization transfer in tissue. *Magn Reson Med* **1995**;33:474–482.
10. Spiller M, Kasoff SS, Lansen TA, et al. Variation of the magnetic relaxation rate 1/T1 of water protons with magnetic field strength (NMRD profile) of untreated, noncalcified, human astrocytomas: correlation with histology and solids content. *J Neuro-Oncol* **1994**;21:113–125.
11. Kasoff SS, Spiller M, Valsamis MP, et al. Relaxometry of non-calcified human meningiomas: correlation with histology and solids content. *Invest Radiol* **1995**;30:49–55.
12. Tenner MS, Spiller M, Koenig SH, et al. Calcification can shorten T2, but not T1, at magnetic resonance imaging fields: results of a relaxometry study of calcified human meningiomas. *Invest Radiol* **1995**;30:345–353.
13. Koenig SH, Brown RD III, Spiller M, Lundbom N. Relaxometry of brain: why white matter is white in MRI. *Magn Reson Med* **1990**;14:482–495.
14. Koenig SH. Cholesterol of myelin is the determinant of gray-white contrast in MRI of brain. *Magn Reson Med* **1991**;20:285–291.
15. Normal and pathological brain iron (whole issue). *J Neurolog Sci* **1995**;134[suppl]:1–114.
16. Koenig SH, Brown RD III. Field-cycling relaxometry of protein solutions and tissue: implications for MRI. *Progr NMR Spectr* **1991**;22:487–565.
17. Koenig SH. Theory of relaxation of mobile water protons by protein NH moieties, with application to rat heart muscle and calf lens homogenates. *Biophys J* **1988**;53:91–96.
18. Koenig SH, Brown RD III, Pande A, Ugolini R. Rotational inhibition and magnetization transfer in α-crystallin solutions. *J Magn Reson* **1993**;B101:172–177.
19. Lindstrom TD, Koenig SH, Boussios T, Bertles JF. Intermolecular interactions of oxygenated sickle hemoglobin in cells and cell-free solutions. *Biophys J* **1976**;19:679–689.
20. Koenig SH, Schillinger WE. Nuclear magnetic relaxation dispersion in protein solutions: 1. Apotransferrin. *J Biol Chem* **1969**;244:3283–3289.
21. Wolff SD, Balaban RS. Magnetization transfer contrast (MTC) in tissue water proton relaxation in vivo. *Magn Reson Med* **1989**;10:135–144.
22. Bloch F, Hansen WW, Packard M. Nuclear induction. *Phys Rev* **1946**; 69:127.
23. Purcell EM, Torrey HC, Pound RV. Resonance absorption by nuclear magnetic moments in a solid. *Phys Rev* **1946**;69:37–39.
24. Koenig SH. Classes of hydration sites at protein-water interfaces: the source of contrast in magnetic resonance imaging. *Biophys J* **1995**; 69:593–603.
25. Cheng X, Schoenborn BP. Hydration in protein crystals: a neutron diffraction study of carbonmonoxymyoglobin crystals. *Acta Cryst* **1990**; B46:195–208.
26. Brown RD III, Koenig SH. 1/T1ρ and low field 1/T1 of tissue water protons arise from magnetization transfer to macromolecular solid-state broadened lines. *Magn Reson Med* **1992**;28:145–152.

Announcements

The University of Michigan Medical School, Department of Radiology, is sponsoring the **18th Annual Seminar in Diagnostic Ultrasound**, which will be held September 19 and 20, 1996, at the Towsley Center at the University of Michigan Medical Center in Ann Arbor. Fifteen hours of Category 1 credit of the Physician's Recognition Award of the American Medical Association will be awarded. Other credits may apply. The course director is Terry M. Silver, MD, FACR.

For more information, contact the Registrar, Towsley Center for Continuing Education, Department of Postgraduate Medical Education, Department of Postgraduate Medicine and Health Care Professions, P.O. Box 1157, Ann Arbor, MI 48106-1157; (313) 763-1400, fax (313) 936-1641.

The University of Michigan Medical School, Department of Radiology, is sponsoring **Advances in Body CT and MRI**, which will be held September 17 and 18, 1996, at the Towsley Center at the University of Michigan Medical Center in Ann Arbor. Category 1 credits to be announced. Other credits may apply. The course director is Melvyn Korobkin, MD.

For more information, contact the Registrar, Towsley Center for Continuing Education, Department of Postgraduate Medical Education, Department of Postgraduate Medicine and Health Care Professions, P.O. Box 1157, Ann Arbor, MI 48106-1157; (313) 763-1400, fax (313) 936-1641.